CSMech

Computation and Simulation in Mechanical Sciences (CSMech)

Elastoplastic dynamic buckling of rectangular plates subjected to impulsive loading with various boundary conditions using deformation and incremental theory of plasticity

H. Ramezannezhad Azarboni

M. Darvizeh

ORIGINAL PAPER

Open Access

Volume: 01

Issue: 01

Winter 2018

Page: 29-41

ISSN:

eISSN:

www.csmech.iaubanz.ac.ir

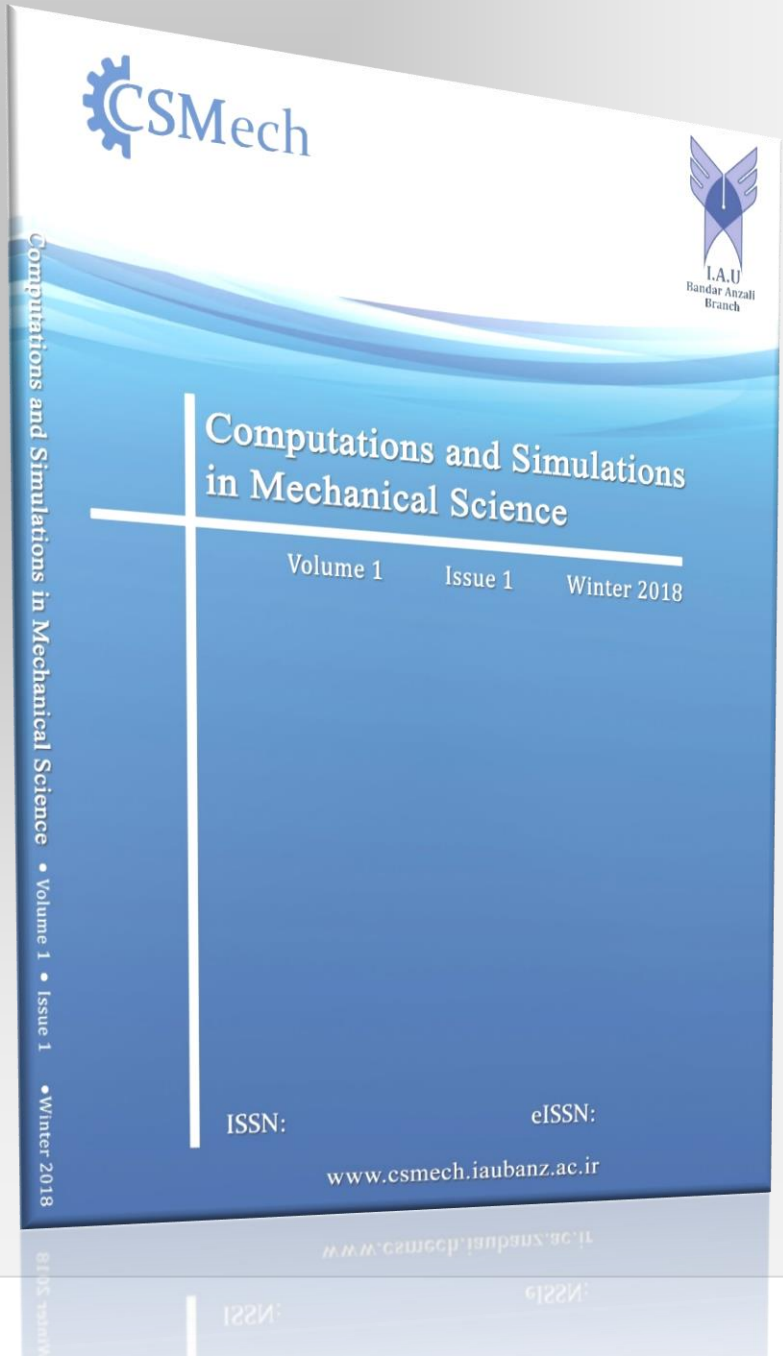

CSMech. **01**(01), 29-41, (2018)

Computations and Simulations in Mechanical Science

ORIGINAL PAPER

CSMech

www.csmech.iaubanz.ac.ir

Elastoplastic dynamic buckling of rectangular plates subjected to impulsive loading with various boundary conditions using deformation and incremental theory of plasticity

H. Ramezannezhad Azarboni [a,*], M. Darvizeh [b]

[a] *Department of Mechanical Engineering, Ramsar branch, Islamic Azad University, Ramsar, Iran*

[b] *Department of Mechanical Engineering, University of Guilan, P.O. Box 3756, Rasht, Iran*

Abstract

The elastoplastic dynamic buckling of a thin rectangular plate with different boundary conditions subjected to uni- and biaxial compression sinusoidal pulse functions is investigated employing Galerkin method on the basis of trigonometric mode shape functions. The equilibrium, stability and dynamic elastoplastic buckling equations are derived based on two theories of plasticity: deformation theory of plasticity (DT) with Hencky constitutive relations and incremental theory of plasticity (IT) with Prandtl-Reuss constitutive relations. Ramberg-Osgood stress-strain model is used to describe the elastoplastic material property of plate. The effects of boundary conditions, force pulse amplitude, loading ratio and type of plasticity theory on the velocity and deflection histories of plate are investigated. According to the dynamic response of plate, the results obtained from DT are lower than those predicted through IT and the boundary conditions of rectangular plate subjected to impulsive load have a significant influence on the dynamic response of palte. The resistance against deformation for corresponding to plates with clamped boundary condition is more than those plates with simply supported boundary condition.

Article history

Received: 2017-12-15
Revised: 2018-01-19
Accepted: 2018-02-25

Keywords

Dynamic Elastoplastic Buckling
Rectangular Plate
Deformation Theory
Incremental Theory
Galerkin Method

1. Introduction

Nowadays, availability, durability, reliability, weight and strength, as the most important factors in optimum engineering design, are responsible for the widespread applications of plates in industry. In order to achieve an optimal design, mechanical properties and behavior of such structures in the presence of different loading conditions should be carefully investigated. Three types of loads, including lateral, axial and combined axial and lateral, can be applied to a plate. Due to the importance of buckling phenomena in the optimum design of plate, extensive buckling analysis has been carried out in elastic or elastoplastic regime. These researches can be classified into two main categories, i.e. static buckling and dynamic buckling [1-34]. Many investigations were carried out in order to analyze the elastoplastic buckling of plates through plasticity theories, i.e. DT and IT. Comparison between experimental and analytical results indicates that DT and IT were applicable in plastic buckling problems. According to these researches, in the case of cylinders subjected to torsional or compressive loads, IT provides more accurate results compared to those of DT, while in long simply supported plates DT predicts better load buckling than IT. For example, the inelastic buckling of infinitely long square simply supported plates, and considering the effects of transverse shear and employing both DT and IT was studied by Shrivastava [10]. Ore and Durban [11] perused the linear elastoplastic buckling of the annular plate under shear loads with both DT and IT. Application of both theories of plasticity in elastoplastic buckling of rectangular plate subjected to uniform compression combined with uniform tension (or compression) in the

*Corresponding author: Tel/Fax: +98 1155260531
E-mail address: h.ramezannejad@iauramsar.ac.ir

perpendicular direction with various types of boundary conditions was studied by Durban and Zuckerman [12]. They found out that in the case of thin plates, DT and IT have the same results, whereas for thicker plates, DT predicts more accurate response compared to IT. According to the published literature, the studies on the buckling behavior of plates have been limited to static ones in the case of elastoplastic rectangular plates. Also, considering the dynamic buckling behavior, it can be observed that narrow investigations have been carried out in elastic regime [13-15]. Moreover, the effects of Ramberg-Osgood coefficient, geometric parameters and boundary conditions on the critical buckling load were explored in the case of thick rectangular and circular elastoplastic plates throughout DT and IT by Chakrabarty et al. [16]. They reported that by increasing the thickness of plates, E/σ_0 and c values of Ramberg-Osgood relation, the divergence of estimated values obtained by both theories increases. Considering the wave propagation, the effect of the impact velocity and striking mass on the development of buckling shape on the dynamic elastic plastic buckling of thin-walled square tubes was investigated by Karagiozova and Jones [17]. Using the semi-analytical complex finite strip method, the inelastic local buckling of flat plate structures that contain plates with variable thicknesses was studied by azhari et al. [18]. Considering DT and IT, Wang et al. [19-20] discussed the effect of Ramberg-Osgood coefficient, geometric parameters and boundary conditions on the plastic buckling in the case of thick rectangular and circular elastoplastic plates. Lotfi et al. [21] investigated the skew isotropic plates subjected to in-plane loadings employing the stability analysis based on the isoparametric spline finite strip method, which includes inelasticity. The elastoplastic buckling investigation of simply supported square and rectangular thin steel plates having elliptic cut-outs using finite element methods were worked by Komur [22]. Inelastic stress distributions, load transfers and failure modes for a range of size and spacing by using inelastic large displacement isoparametric spline finite strip method were investigated by Yao and Rasmussen [23]. Tang and Li [24] experimentally studied the axial dynamic buckling responses of pseudo-elastic NiTi alloy cylindrical shells for various lengths/diameter ratios and end constraint conditions by using a modified single pulse SHPB apparatus. The axisymmetrical buckling and non-axisymmetric buckling modes were discussed. Fyllingen et al. [25] studied on the transition from progressive buckling to global bending during axial crushing of long square tubes experimentally. The propagation of buckling at the end of the tube and observation of deformation modes were discussed. By applying the numerical nonlinear finite element method and theoretical p-Ritz energy method the inelastic buckling and postbuckling behavior of stocky plates under combined shear and in-plane bending stresses were developed and compared to slender plates by Alinia et al. [26]. Douville and Grognec [27] carried out the elastic buckling analyses of classical sandwich beam-columns in order to derive the critical values and the associated bifurcation modes under various loadings analytically. Using the generalized differential quadrature (GDQ) discretization technique in DT and IT, the elastoplastic buckling of a thin rectangular plate with various boundary conditions was investigated by Kadkhodayan and Maarefdoust [28-29]. The difference between the results obtained by these two theories and the effects of the geometrical parameters and boundary conditions were discussed. Considering the incremental theory of plasticity and the deformation theory of plasticity, the plastic buckling of circular cylindrical shells under axial compression was investigated by shamass et al. [30]. Trybula and Krzelecki [31] discussed the modification of postbuckling path concept by application of additional loadings acting on the structure without changing the shape or sizes of the optimized element. ANSYS code was used for calculations of elastic–plastic shells of geometry and loading. Gumruk [32] studied the dynamic plastic buckling behavior of an aluminum alloy cylindrical shell with an axial linear variable thickness, discontinuity and conical shaped for high velocity impact using finite element method. Picandet et al. [33] carried out the buckling and postbuckling of a perfect axially loaded column analytically through a global bilinear moment-curvature elastoplastic constitutive law. Elastoplastic dynamic buckling analysis of rectangular plate subjected to impulsive loading with different

boundary conditions leads to complex coupled equations to solve. For this reason, the elastoplastic buckling analysis of rectangular plates is limited to derive the critical buckling load and very limited dynamic buckling analyses have been performed so far for the rectangular plates .Employing DT and IT for dynamic buckling behavior analysis of elastoplastic rectangular plate subjected to uni- and biaxial compressive sinusoidal pulse function by applying Galerkin method along with the trigonometric shape functions for different boundary conditions is the innovation of this paper. To this end, initially, by using DT with the Hencky constitutive relations and IT with the Prandtl-Reuss constitutive relations, the equilibrium, stability and dynamic elastoplastic buckling equations for rectangular plate are derived. Then, the Ramberg-Osgood stress-strain model is selected to describe the elastoplastic material property of plate. Finally, the effects of different boundary conditions, force pulse amplitude, geometrical parameter and type of plasticity theory on the velocity and deflection histories of plate are investigated.

2. Governing equations

Considering the Mindlin theory of plate, the admissible field velocity can be written as [34]

$$v_x = \dot{u} - z\frac{\partial \dot{w}}{\partial x} \tag{1a}$$

$$v_y = \dot{v} - z\frac{\partial \dot{w}}{\partial y} \tag{1b}$$

$$v_z = \dot{w} \tag{1c}$$

where u, v and w represent the deflection of the middle surface of plate about the $x, y$and z directions, respectively. According to field velocity, the strain rates are given by

$$\dot{\varepsilon}_{xx} = \frac{\partial \dot{u}}{\partial x} - z\frac{\partial^2 \dot{w}}{\partial x^2} \tag{2a}$$

$$\dot{\varepsilon}_{yy} = \frac{\partial \dot{v}}{\partial y} - z\frac{\partial^2 \dot{w}}{\partial y^2} \tag{2b}$$

$$\dot{\varepsilon}_{xx} = \frac{1}{2}\left(\frac{\partial \dot{u}}{\partial y} + \frac{\partial \dot{v}}{\partial x}\right) - 2z\frac{\partial^2 \dot{w}}{\partial x \partial y} \tag{2c}$$

2.1. Deformation theory (DT) based on Hencky equation

The Hencky equation for plastic strain is given as follows [34]

$$\varepsilon_{ij}^p = \frac{3\bar{\varepsilon}^p}{2\bar{\sigma}} S_{ij} \tag{3}$$

where $\bar{\varepsilon}^p, \bar{\sigma}$ and S_{ij} are the effective plastic strain, effective stress and deviatoric stress vector, respectively. The rate of plastic strain equation in the incremental form is obtained by differentiating of Eq. (3) with respect to time as.

$$d\varepsilon_{ij}^p = \frac{3d\bar{\sigma}}{2\bar{\sigma}}\left(\frac{d\bar{\varepsilon}^p}{d\bar{\sigma}} - \frac{\bar{\varepsilon}^p}{\bar{\sigma}}\right) S_{ij} + \frac{3\bar{\varepsilon}^p}{2\bar{\sigma}} dS_{ij} \tag{4}$$

where dS_{ij} represents the time increment of the deviatoric stress vector. Based on Hook's law, the strain-stress relation for elastic deformation can be written in tensorial notation by Eq. (5)

$$\varepsilon_{ij}^e = \frac{1+\nu}{E} S_{ij} + \frac{1-2\nu}{3E}\delta_{ij}\sigma_{kk} \tag{5}$$

The incremental form of Eq. (5) is derived as

$$d\varepsilon_{ij}^e = \frac{1+\nu}{E} dS_{ij} + \frac{1-2\nu}{3E}\delta_{ij} d\sigma_{kk} \tag{6}$$

where ν is the Poisson's ratio, E denotes the young's module and δ_{ij} expresses the Kronecker delta. The complete elastic-plastic stress-strain relation is obtained by combination of Eqs. (4) and (6)

$$E\dot{\varepsilon}_{ij} = \left(\frac{3E}{2E_s} - \frac{1-2\nu}{2}\right)\dot{S}_{ij} + \left(\frac{1-2\nu}{3}\right)\dot{\sigma}_{kk}\delta_{ij} + \frac{3\dot{\bar{\sigma}}}{2\bar{\sigma}}\left(\frac{E}{E_t} - \frac{E}{E_s}\right) S_{ij} \tag{7}$$

In Eq. (7), $E_t = \frac{d\bar{\sigma}}{d\bar{\varepsilon}}$ and $E_s = \frac{\bar{\sigma}}{\bar{\varepsilon}}$ indicate the tangent and secant module, respectively where $\bar{\varepsilon}$ is the total effective strain. Consider a thin rectangular plate with length a, width b, uniform thickness h and exposed uniform axial compressive stress σ. According to the Von-Mises yield criterion, the effective stress is defined as

$$\bar{\sigma} = \sqrt{\sigma_x^2 - \sigma_x\sigma_y + \sigma_y^2 + 3\sigma_{xy}^2} \tag{8}$$

By applying the straightforward differentiation to Eq. (8) and substituting the principle stress, the following equation can be derived.

$$\frac{\dot{\bar{\sigma}}}{\bar{\sigma}} = -\frac{(2\sigma_1 - \sigma_2)\dot{\sigma}_x + (2\sigma_2 - \sigma_1)\dot{\sigma}_y}{2\bar{\sigma}^2} \tag{9}$$

Substituting Eq. (9) into Eq. (7) and then extending in the Cartesian coordinate for isotropic materials, the strain rate relation in terms of stress rate can be derived.

$$E_t\dot{\varepsilon}_x = \left[1 - \frac{3}{4}\left(1 - \frac{E_t}{E_s}\right)\frac{\sigma_2^2}{\bar{\sigma}^2}\right]\dot{\sigma}_x - \left[\vartheta - \frac{3}{4}\left(1 - \frac{E_t}{E_s}\right)\frac{\sigma_1\sigma_2}{\bar{\sigma}^2}\right]\dot{\sigma}_y \tag{10a}$$

$$E_t\dot{\varepsilon}_y = \left[1-\frac{3}{4}\left(1-\frac{E_t}{E_s}\right)\frac{\sigma_1^2}{\bar{\sigma}^2}\right]\dot{\sigma}_y - \left[\vartheta-\frac{3}{4}\left(1-\frac{E_t}{E_s}\right)\frac{\sigma_1\sigma_2}{\bar{\sigma}^2}\right]\dot{\sigma}_x \quad (10b)$$

where ϑ is the contraction ratio and can be expressed in terms of ν, E and E_t by Eq. (11)

$$\vartheta = \frac{1}{2}-\frac{(1-2\nu)E_t}{2E} \quad (11)$$

The stress rate-strain rate relation can be derived by inversion of Eqs. (10a) and (10b) asfollows [34]

$$\dot{\sigma}_x = E\left[\alpha\dot{\varepsilon}_{xx}+\beta\dot{\varepsilon}_{yy}\right] \quad (12a)$$

$$\dot{\sigma}_y = E\left[\beta\dot{\varepsilon}_{xx}+\gamma\dot{\varepsilon}_{yy}\right] \quad (12b)$$

$$\dot{\sigma}_{xy} = 2G\dot{\varepsilon}_{xy} \quad (12c)$$

where

$$\alpha = \frac{1}{\lambda}\left[4-3\left(1-\frac{E_t}{E_s}\right)\frac{\sigma_1^2}{\bar{\sigma}^2}\right] \quad (13a)$$

$$\beta = \frac{1}{\lambda}\left[2-2(1-2\nu)\frac{E_t}{E}-3\left(1-\frac{E_t}{E_s}\right)\frac{\sigma_1\sigma_2}{\bar{\sigma}^2}\right] \quad (13b)$$

$$\gamma = \frac{1}{\lambda}\left[4-3\left(1-\frac{E_t}{E_s}\right)\frac{\sigma_2^2}{\bar{\sigma}^2}\right] \quad (13c)$$

$$\lambda = \frac{3E}{E_s}+(1-2\nu)\left[2-(1-2\nu)\frac{E_t}{E}-3\left(1-\frac{E_t}{E_s}\right)\frac{\sigma_1\sigma_2}{\bar{\sigma}^2}\right] \quad (13d)$$

$$\frac{E}{G} = 2+2\nu+3\left(\frac{E}{E_s}-1\right) \quad (13e)$$

By considering the effective stress in terms of σ_x, σ_y and σ_{xy}, the strain rate-stress rate relation can be written as [17]

$$E_t\begin{Bmatrix}\dot{\varepsilon}_{xx}\\ \dot{\varepsilon}_{yy}\\ \dot{\varepsilon}_{xy}\end{Bmatrix} = [K]\begin{Bmatrix}\dot{\sigma}_{xx}\\ \dot{\sigma}_{yy}\\ \dot{\sigma}_{xy}\end{Bmatrix} \quad (14)$$

where the matrix elements are given by

$$k_{11} = \left[1-3\left(1-\frac{E_t}{E_s}\right)\left(\frac{\sigma_y^2}{4\bar{\sigma}^2}+\frac{\sigma_{xy}^2}{\bar{\sigma}^2}\right)\right] \quad (15a)$$

$$k_{12} = k_{21} = -\frac{1}{2}\left[1-(1-2\nu)\frac{E_t}{E}-3\left(1-\frac{E_t}{E_s}\right)\left(\frac{\sigma_x\sigma_y}{2\bar{\sigma}^2}+\frac{\sigma_{xy}^2}{\bar{\sigma}^2}\right)\right] \quad (15b)$$

$$k_{13} = k_{13} = \frac{3}{2}\left[\left(1-\frac{E_t}{E_s}\right)\left(\frac{2\sigma_x-\sigma_y}{\bar{\sigma}}\right)\left(\frac{\sigma_{xy}}{\bar{\sigma}}\right)\right] \quad (15c)$$

$$k_{22} = \left[1-3\left(1-\frac{E_t}{E_s}\right)\left(\frac{\sigma_x^2}{4\bar{\sigma}^2}+\frac{\sigma_{xy}^2}{\bar{\sigma}^2}\right)\right] \quad (15d)$$

$$k_{23} = k_{32} = \frac{3}{2}\left[\left(1-\frac{E_t}{E_s}\right)\left(\frac{2\sigma_y-\sigma_x}{\bar{\sigma}}\right)\left(\frac{\sigma_{xy}}{\bar{\sigma}}\right)\right] \quad (15e)$$

$$k_{33} = \frac{3E_t}{E_s}-(1-2\nu)\frac{E_t}{E}+9\left(1-\frac{E_t}{E_s}\right)\left(\frac{\sigma_{xy}^2}{\bar{\sigma}^2}\right) \quad (15f)$$

The stress rate-strain rate relation can be derived by inversion of Eq. (14)

$$E\begin{Bmatrix}\dot{\sigma}_{xx}\\ \dot{\sigma}_{yy}\\ \dot{\sigma}_{xy}\end{Bmatrix} = \begin{bmatrix}\alpha & \beta & \chi\\ \beta & \gamma & \mu\\ \chi & \mu & \delta\end{bmatrix}\begin{Bmatrix}\dot{\varepsilon}_{xx}\\ \dot{\varepsilon}_{yy}\\ \dot{\varepsilon}_{xy}\end{Bmatrix} \quad (16)$$

where

$$\alpha = \frac{1}{\lambda}[k_{22}k_{33}-k_{23}^2] \quad (17a)$$

$$\beta = \frac{1}{\lambda}[k_{13}k_{23}-k_{12}k_{33}] \quad (17b)$$

$$\chi = \frac{1}{\lambda}[k_{12}k_{23}-k_{13}k_{22}] \quad (17c)$$

$$\gamma = \frac{1}{\lambda}[k_{11}k_{33}-k_{13}^2] \quad (17d)$$

$$\mu = \frac{1}{\lambda}[k_{12}k_{13}-k_{11}k_{23}] \quad (17e)$$

$$\delta = \frac{1}{\lambda}[k_{11}k_{22}-k_{12}^2] \quad (17f)$$

$$\lambda = \frac{E}{E_t}|K| \quad (17g)$$

2.2. Incremental theory (IT) based on Prandtl–Reuss equation

The constitutive relations for material that obey from Von-Mises yield criterion and the associated Prandtl-Reuss flow rule can be obtained as [16]

$$\dot{\varepsilon}_{ij}^p = \frac{3\dot{\bar{\sigma}}}{2\bar{\sigma}}\left(\frac{1}{E_t}-\frac{1}{E}\right) \quad (18)$$

The complete elastic-plastic stress-strain relation is obtained by combination of Eqs. (5) and (14) as follows.

$$E\dot{\varepsilon}_{ij} = (1+\nu)\dot{S}_{ij}+\left(\frac{1-2\nu}{3}\right)\dot{\sigma}_{kk}\delta_{ij}+\frac{3\dot{\bar{\sigma}}}{2\bar{\sigma}}\left(\frac{E}{E_t}-1\right)S_{ij} \quad (19)$$

According to deformation theory, the parameters in the stress rate to strain rate relations can be derived as [34]

$$\alpha = \frac{1}{\lambda}\left[4-3\left(1-\frac{E_t}{E}\right)\frac{\sigma_1^2}{\bar{\sigma}^2}\right] \quad (20a)$$

$$\beta = \frac{1}{\lambda}\left[2-2(1-2\nu)\frac{E_t}{E}-3\left(1-\frac{E_t}{E}\right)\frac{\sigma_1\sigma_2}{\bar{\sigma}^2}\right] \quad (20b)$$

$$\gamma = \frac{1}{\lambda}\left[4-3\left(1-\frac{E_t}{E}\right)\frac{\sigma_2^2}{\bar{\sigma}^2}\right] \quad (20c)$$

$$\lambda = (5-4\nu)+(1-2\nu)^2\frac{E_t}{E}-3(1-2\nu)\left(1-\frac{E_t}{E}\right)\frac{\sigma_1\sigma_2}{\bar{\sigma}^2} \quad (20d)$$

$$\frac{E}{G} = 2(1+\nu) \quad (20e)$$

The strain rate - stress rate matrix element relation, by considering the incremental theory based on Prandtl–Reuss equation can be derived as [28, 29]

$$k_{11} = \left[1-3\left(1-\frac{E_t}{E}\right)\left(\frac{\sigma_y^2}{4\bar{\sigma}^2}+\frac{\sigma_{xy}^2}{\bar{\sigma}^2}\right)\right] \quad (21a)$$

$$k_{12} = k_{21} = -\frac{1}{2}\left[1-(1-2\nu)\frac{E_t}{E}-3\left(1-\frac{E_t}{E}\right)\left(\frac{\sigma_x\sigma_y}{2\bar{\sigma}^2}+\frac{\sigma_{xy}^2}{\bar{\sigma}^2}\right)\right] \quad (21b)$$

$$k_{13} = k_{13} = \frac{3}{2}\left[\left(1-\frac{E_t}{E}\right)\left(\frac{2\sigma_x-\sigma_y}{\bar{\sigma}}\right)\left(\frac{\sigma_{xy}}{\bar{\sigma}}\right)\right] \quad (21c)$$

$$k_{22} = \left[1-3\left(1-\frac{E_t}{E}\right)\left(\frac{\sigma_x^2}{4\bar{\sigma}^2}+\frac{\sigma_{xy}^2}{\bar{\sigma}^2}\right)\right] \quad (21d)$$

$$k_{23} = k_{32} = \frac{3}{2}\left[\left(1-\frac{E_t}{E}\right)\left(\frac{2\sigma_y-\sigma_x}{\bar{\sigma}}\right)\left(\frac{\sigma_{xy}}{\bar{\sigma}}\right)\right] \quad (21e)$$

$$k_{33} = \frac{3E_t}{E_s}-(1-2\nu)\frac{E_t}{E}+9\left(1-\frac{E_t}{E}\right)\left(\frac{\sigma_{xy}^2}{\bar{\sigma}^2}\right) \quad (21f)$$

The Ramberg-Osgood stress-strain model is used to describe the elastoplastic material property of plate. The Ramberg-Osgood constitutive law is defined as

$$\varepsilon = \frac{\bar{\sigma}}{E}+k\left(\frac{\bar{\sigma}}{E}\right)^c \quad (22)$$

where $\varepsilon, \bar{\sigma}, k, c$ representthe total strain, equivalent stress and material parameters, respectively. According to Eq. (22) and considering the tangent and secant modulus which are respectively defined as $E_t = \frac{d\bar{\sigma}}{d\bar{\varepsilon}}$ and $E_s = \frac{\bar{\sigma}}{\bar{\varepsilon}}$, these parameters are derived as follows [12]

$$\frac{E}{E_t} = 1+ck\left(\frac{\bar{\sigma}}{E}\right)^{c-1}$$
$$\frac{E}{E_s} = 1+k\left(\frac{\bar{\sigma}}{E}\right)^{c-1} \quad (23)$$

2.3 Governing equation elastic/plastic dynamic buckling of thin plate

The strain energy for a rectangular plate is given by [16]

$$U_s = \frac{1}{2}\int \dot{\sigma}_{ij}\dot{\varepsilon}_{ij}dV = \frac{1}{2}\iiint\left(\dot{\sigma}_{xx}\dot{\varepsilon}_{xx}+\dot{\sigma}_{yy}\dot{\varepsilon}_{yy}+\dot{\sigma}_{xy}\dot{\varepsilon}_{xy}\right)dxdydz \quad (24)$$

Also, by neglecting the rotational inertia and assuming the transverse motion, the kinetic energy of the plate can be expressed as follows.

$$K_t = \frac{\rho h}{2}\iint_A\left(\frac{\partial w}{\partial t}\right)^2 dA \quad (25)$$

By considering the external uniform in-plane compressive and shear stress applied to plate, the potential energy can be written as follows.

$$W = -\frac{1}{2}\iiint \dot{\sigma}_{xx}w_x^2+\dot{\sigma}_{yy}w_{y+}^2 2\dot{\sigma}_{xy}w_xw_ydxdydz \quad (26)$$

and then by applying the Hamilton principle as given below.

$$\delta\left(\int_{t_0}^{t_1}(K_t-U_s+W)dt\right) = 0 \quad (27)$$

By applying varaitional method the elastoplastic equation of motion for the lateral deflection can be derived.

$$\alpha\frac{\partial^4 w}{\partial x^4}+4\chi\frac{\partial^4 w}{\partial x^3\partial y}+2(\beta+2\delta)\frac{\partial^4 w}{\partial x^2\partial y^2}+4\mu\frac{\partial^4 w}{\partial x\partial y^3}+\gamma\frac{\partial^4 w}{\partial y^4}+\frac{12}{h^2E}(\sigma_{xx}\frac{\partial^2 w}{\partial x^2}+\sigma_{yy}\frac{\partial^2 w}{\partial y^2}+2\sigma_{xy}\frac{\partial^2 w}{\partial x\partial y})+\rho h\frac{\partial^2 w}{\partial t^2} = 0 \quad (28)$$

3. Solution methodology

Three types of functions can be used to solve the nonlinear dynamic buckling problem of plate, i.e. admissible, comparison and eigen functions. Any arbitrary function that satisfies all the geometric boundary conditions of the eigenvalue problem which is R times differentiable over domain Scan be considered as the admissible function. Moreover, any arbitrary function that satisfies all the geometric and natural boundary conditions of the eigenvalue problem and is 2R times differentiable over domain S can be considered as the comparison functions. Eigen functions satisfy all the boundary conditions and the differential equation of the eigenvalue problem. In this study, to solve Eq. (28), the linear combinations of admissible functions in series form are employed. These functions can be used for geometric function, $w(x,y,t)$. In general, these functions can be considered as follow

$$w(x,y,t) = \sum\sum W_{mn}(t)\Psi_m(x)\Phi_n(y) \quad (29)$$

The Eq(29) satisfies all the geometric and natural boundary conditions. By substituting Eq.(29) into elastoplastic equation of motion for the lateral deflection, Eq. (28) can be rewritten as

$$\sum\sum[\alpha W_{mn}(t)\frac{d^4\Psi_m(x)}{dx^4}\Phi_n(y)+4\chi W_{mn}(t)\frac{d^3\Psi_m(x)}{dx^3}\frac{d\Phi_n(y)}{dy}+2(\beta+2\delta)W_{mn}(t)\frac{d^2\Psi_m(x)}{dx^2}$$

$$\frac{d^2\Phi_n(y)}{dy^2} + 4\mu W_{mn}(t)\frac{d\Psi_m(x)}{dx}\frac{d^3\Phi_n(y)}{dy^3} + \gamma W_{mn}(t)\Psi_m(x)\frac{d^4\Phi_n(y)}{dy^4} + \frac{12}{h^2E}(\sigma_{xx}W_{mn}(t)\Phi_n(y) \frac{d^2\Psi_m(x)}{dx^2} + \sigma_{yy}W_{mn}(t)\Psi_m(x)\frac{d^2\Phi_n(y)}{dy^2} + 2\sigma_{xy}W_{mn}(t)\frac{d\Psi_m(x)}{dx}\frac{d\Phi_n(y)}{dy}) + \rho h\frac{d^2W_{mn}(t)}{dt^2}\Psi_m(x)$$

$$\Phi_n(y) = 0 \quad (30)$$

By substituting admissible functions of six different boundary conditions in the membrane force equation and multiplying achieved equation in $\Psi_r(x)\Phi_s(y)$ and finally using Galerkin procedure over the plan area, a first-order ordinary differential equation is achieved as.

$$\sum_{m=1}^{M}\sum_{n=1}^{N}\sum_{r=1}^{M}\sum_{s=1}^{N}\{[\alpha\Gamma^1_{mnrs} + 4\chi\Gamma^2_{mnrs} + 2(\beta+2\delta)\Gamma^3_{mnrs} + 4\mu\Gamma^4_{mnrs} + \gamma\Gamma^5_{mnrs} + \frac{12}{h^2E}(\sigma_{xx}\Gamma^6_{mnrs} + \sigma_{yy}\Gamma^7_{mnrs} + 2\sigma_{xy}\Gamma^8_{mnrs})W_{mn}(t) + \rho h\Gamma^9_{mnrs}\frac{d^2W_{mn}(t)}{dt^2} \quad (31)$$

Where

$$\Gamma^1_{mnrs} = \int_0^a(\Psi_m^{xxxx}\Psi_r)\,dx\int_0^b(\Phi_n\Phi_s)dy \quad (32a)$$

$$\Gamma^2_{mnrs} = \int_0^a(\Psi_m^{xxx}\Psi_r)\,dx\int_0^b(\Phi_n^{y}\Phi_s)dy \quad (32b)$$

$$\Gamma^3_{mnrs} = \int_0^a(\Psi_m^{xx}\Psi_r)\,dx\int_0^b(\Phi_n^{yy}\Phi_s)dy \quad (32c)$$

$$\Gamma^4_{mnrs} = \int_0^a(\Psi_m^{x}\Psi_r)\,dx\int_0^b(\Phi_n^{yyy}\Phi_s)dy \quad (32d)$$

$$\Gamma^5_{mnrs} = \int_0^a(\Psi_m\Psi_r)\,dx\int_0^b(\Phi_n^{yyyy}\Phi_s)dy \quad (32e)$$

$$\Gamma^6_{mnrs} = \int_0^a(\Psi_m^{xx}\Psi_r)\,dx\int_0^b(\Phi_n\Phi_s)dy \quad (32f)$$

$$\Gamma^7_{mnrs} = \int_0^a(\Psi_m\Psi_r)\,dx\int_0^b(\Phi_n^{yy}\Phi_s)dy \quad (32g)$$

$$\Gamma^8_{mnrs} = \int_0^a(\Psi_m^{x}\Psi_r)\,dx\int_0^b(\Phi_n^{y}\Phi_s)dy \quad (32h)$$

$$\Gamma^9_{mnrs} = \int_0^a(\Psi_m\Psi_r)\,dx\int_0^b(\Phi_n\Phi_s)dy \quad (32k)$$

4. Results and discussion

The elastoplastic dynamic buckling response of isotropic rectangular plate subjected to pulse load, P_x , with six various types boundary conditions is presented. The pulse load includes sinusoidal and exponential impulse load that is presented in Table. 1, where,T_s is pulse or shock duration and P_x is the amplitude of load.

Table. 1. unidirectional pulse loading function.

Loading type	Function
Sinusoidal	$P = P_x sin\left(\frac{\pi t}{T_s}\right)(1 - H(t - T_s))$

The regime of loading conditions can be determined by the value of shock duration which is dependent on/related to the fundamental flexural natural frequency of the plate. In the cases of impulsive pulse loading, $T \ll T_b/2$ whereT_b is the fundamental flexural natural frequency of the plate. Table. 2 shows the trigonometric admissible functions for six different boundary conditions.

In Table. 2, S and C represent the simply supported and clamped boundary conditions for rectangular plate, correspondingly. The material parameters of the plate are selected to be $E = 72.4GPa$, $\nu = 0.32$ and $\rho = 2700\ Kg/m^3$. The area is $a \times b = 0.3 \times 0.3\ m^2$, the thickness of $h = 0.005\ m$ and the Ramberg-Osgood parameters are equal to $k = 3.94 \times 10^{21}, c = 10.9$ [28].

In order to compare the two theories, IT and DT, the maximum displacement and velocity are changed at the center of fully clamped square plate under uni-and biaxial sinusoidal impulse with respect to time.

Two applied amplitudes of the uni-and biaxial loads are equal to $P_x = 540$ Mpa, $P_x = 560$ Mpa and $P_x = 280$ Mpa, $P_x = 270$ Mpa , respectively. Variations of maximum displacement and velocity versus with the time of fully clamped plate under an impulsive sinusoidal pulse force for different values of loading amplitude by considering both theories of plasticity are shown in Fig. 1 and 2, respectively.

Similar to static analysis, in the elastoplastic dynamic buckling analysis of plate, the results of DT are more accurate than those of IT. Results predicted by DT are in good agreement with those obtained of experimental ones [17]. Also, Fig. 1 and 2 to shows that the maximum displacement under impulsive load is approximately obtained before the pulse is removed and remains constant both in uni- and biaxial impulsive loadings respectively.

Table. 2. Trigonometric admissible functions for six different boundary conditions.

Boundary condition	Function
SSSS	$w(x,y,t)=\sum\sum W_{mn}sin\left(\frac{m\pi x}{a}\right)sin\left(\frac{n\pi y}{b}\right)$
CSSS	$w(x,y,t)=\sum\sum W_{mn}sin\left(\frac{\pi x}{2a}\right)sin\left(\frac{m\pi x}{a}\right)sin\left(\frac{n\pi y}{b}\right)$
CCSS	$w(x,y,t)=\sum\sum W_{mn}sin\left(\frac{\pi x}{a}\right)sin\left(\frac{m\pi x}{a}\right)sin\left(\frac{n\pi y}{b}\right)$
CSCS	$w(x,y,t)=\sum\sum W_{mn}sin\left(\frac{\pi x}{2a}\right)sin\left(\frac{m\pi x}{a}\right)sin\left(\frac{\pi y}{2b}\right)sin\left(\frac{n\pi y}{b}\right)$
CCCS	$w(x,y,t)=\sum\sum W_{mn}sin\left(\frac{\pi x}{a}\right)sin\left(\frac{m\pi x}{a}\right)sin\left(\frac{\pi y}{2b}\right)sin\left(\frac{n\pi y}{b}\right)$
CCCC	$w(x,y,t)=\sum\sum W_{mn}sin\left(\frac{\pi x}{a}\right)sin\left(\frac{m\pi x}{a}\right)sin\left(\frac{\pi y}{b}\right)sin\left(\frac{n\pi y}{b}\right)$

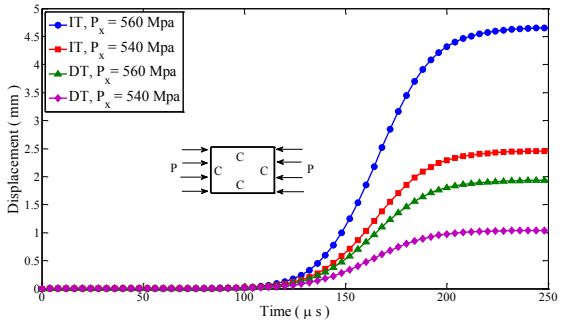

Fig. 1. Comparison of different plasticity theories for deflection history at the center of fully clamped square plate subjected to uniaxial different pulse amplitude

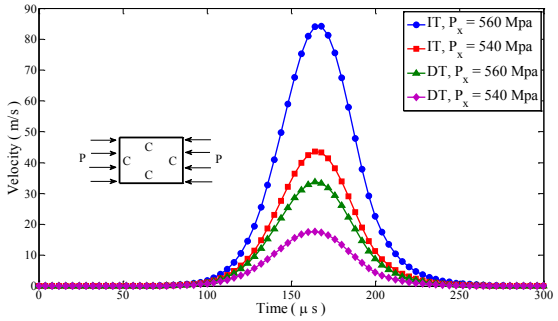

Fig. 3. Comparison of different plasticity theories for velocity history at the center of fully clamped square plate subjected to uniaxial different pulse amplitude

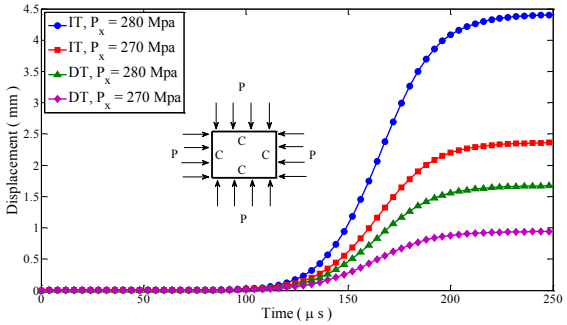

Fig. 2. Comparison of different plasticity theories for deflection history at the center of fully clamped square plate subjected to biaxial different pulse amplitude

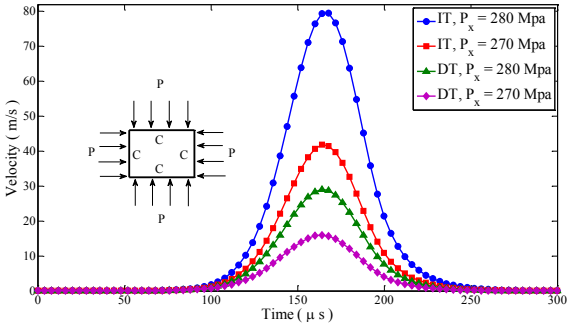

Fig. 4. Comparison of different plasticity theories for velocity history at the center of fully clamped square plate subjected to biaxial different pulse amplitude

As it can be seen in Fig. 3 to 4, the velocity at the center of the plate will be reached the maximum value, approximately, before the loading is released. Then, the plate returns to its static state. Moreover, in order to produce the same velocity and displacement in the biaxial loading, half of the amplitude of impulsive loads in uniaxial case is imposed.

The effect of different boundary conditions on the time history of maximum displacement and plate velocity is shown in Fig. 5 to 8. In order to apply the impulsive load, considering the different boundary conditions, the time duration is selected according to the fundamental flexural natural frequency of the plate. The minimum and maximum values of

fundamental flexural natural frequencies occur in the case of fully clamped and fully simply supported boundary conditions, respectively. So, the time duration of impulsive load for a plate with CCCC, CCCS, CSCS, CCSS, CSSS and SSSS has the lowest values respectively. As shown in Fig. 5 to 8, the maximum displacement and velocity occur approximately before time duration.

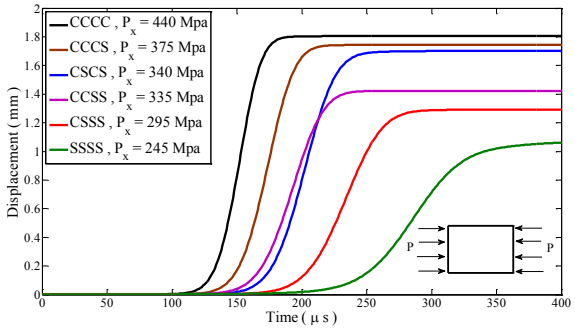

Fig. 5. Effect of different boundary conditions on displacement history at the center of square plate subjected to uniaxial pulse load

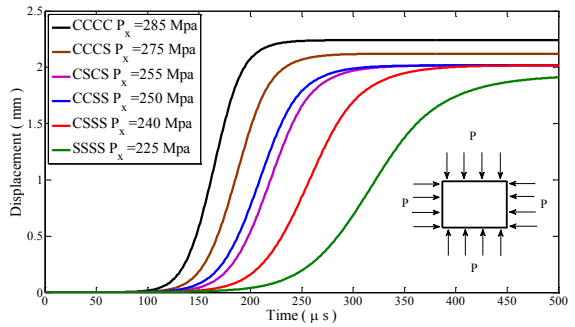

Fig. 6. Effect of different boundary conditions on displacement history at the center of square plate subjected to biaxial pulse load

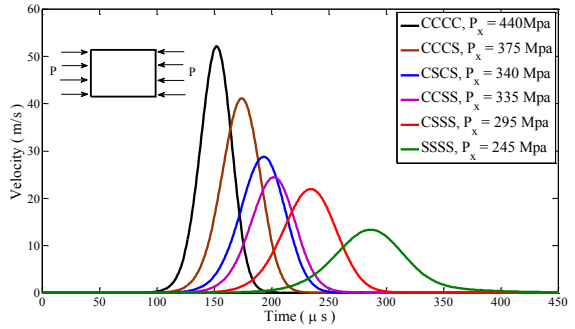

Fig. 7. Effect of different boundary conditions on velocity history at the center of square plate subjected to uniaxial pulse load

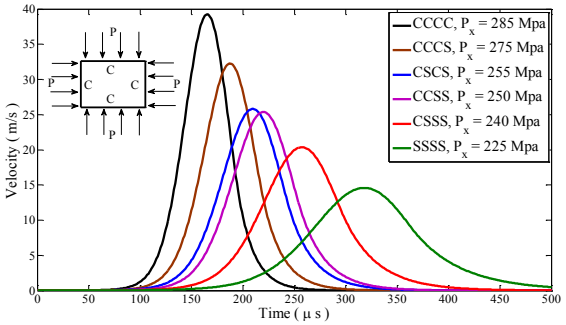

Fig. 8. Effect of different boundary conditions on velocity history at the center of square plate subjected to biaxial pulse load

The effects of the applied amplitude of uniaxial load on the maximum velocity of plate for various boundary conditions are presented in Fig. 9, in order to more precisely study, the velocity of plate is shown in the longitudinal direction from its center.

Based on Fig. 9, decreasing the amplitude of applied load has leads to a reduction in the velocity of plate for all boundary conditions. Moreover, for symmetric boundary conditions such as CCCC, CCSS and SSSS boundary conditions, the velocity of plates along the x and y directions is symmetric, as demonstrated in Figs. 9(a), 9(b) and 9(c). While for asymmetric boundary conditions, the maximum velocity points of plate tend to edges that correspond to the simply supported boundary conditions. This means that the plate resistance against deformation with clamped boundary condition is more than that of plate with simply supported boundary condition. Consequently, the adjacent points to clamped boundary condition have a lower velocity field than those with simply supported boundary condition. This kind of asymmetry in the velocity field can be seen in the plates with CCCS, CSCS and CSSS boundary conditions which are shown in Figs 5(d), 9(e) and 9(f).

In the case of biaxial load, the velocity field of plate with symmetric boundary conditions and asymmetric boundary conditions are presented in Fig. 10 and 11. To clarify symmetric and asymmetric velocity field of plate with different boundary conditions, two-dimensional images of plate are also presented. As shown in Fig. 10, both symmetric boundary conditions and loading conditions result in a symmetrical field of velocity for plates with CCCC, CCSS and SSSS boundary conditions. However, the asymmetric boundary conditions

with symmetric loading conditions lead to the asymmetric velocity field for the square plate with CCCS, CSCS and CSSS boundary conditions which can be seen in Fig. 11.

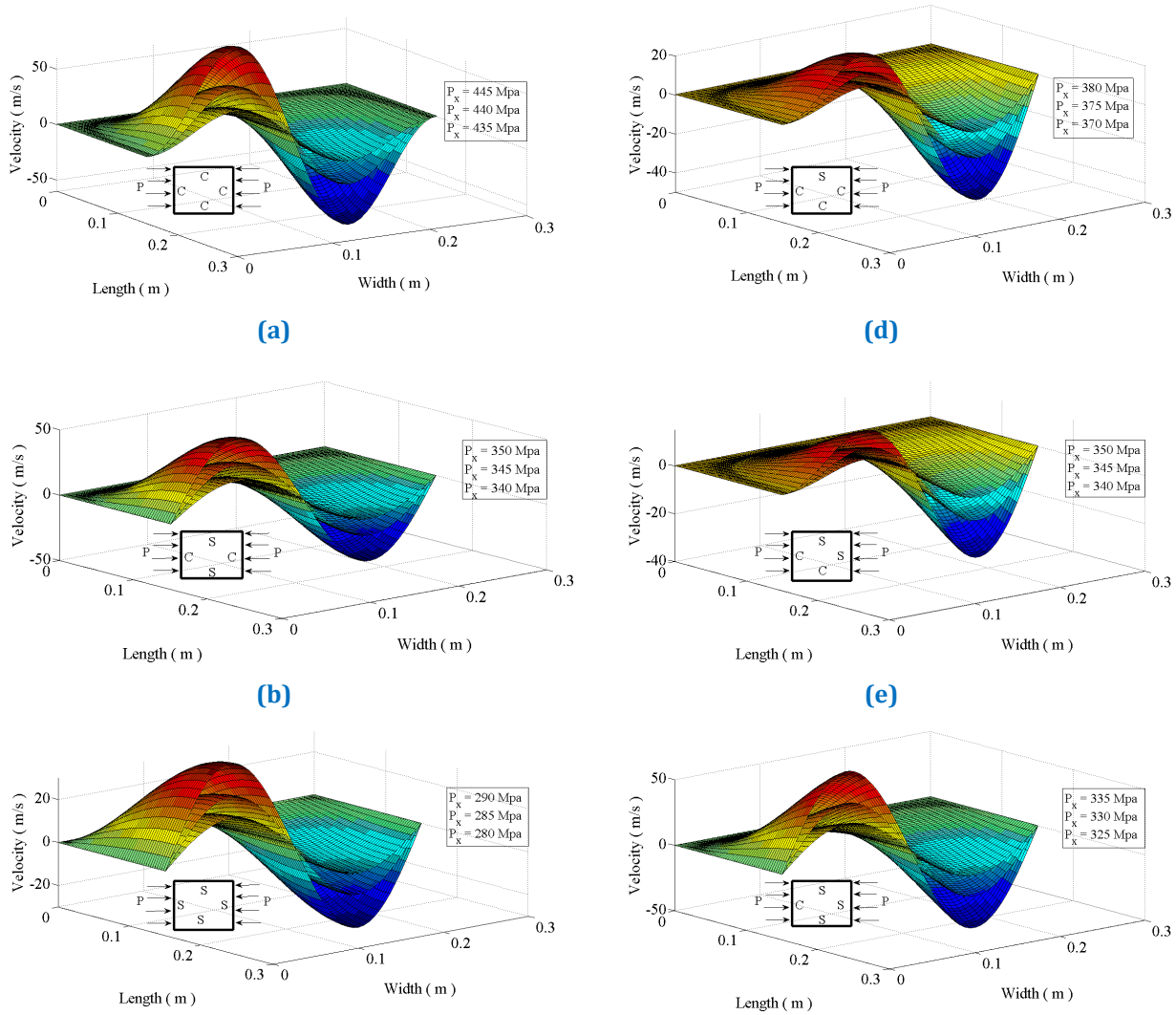

Fig. 9. Maximum velocity field of square plate subjected to uniaxial different pulse amplitude

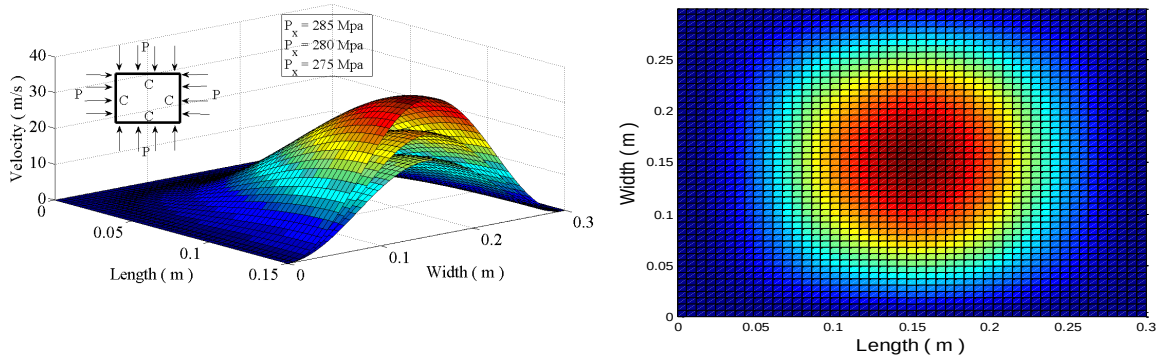

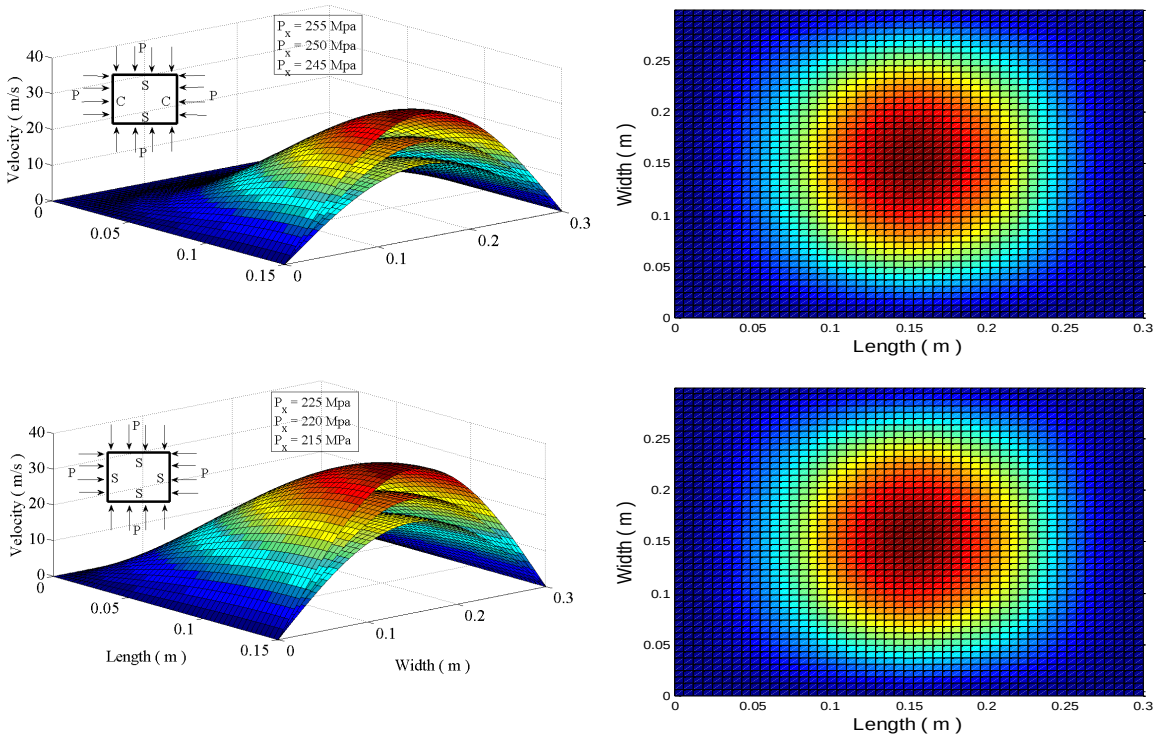

Fig. 10. Maximum velocity field of square plate with symmetric boundary conditions subjected to biaxial different pulse amplitude

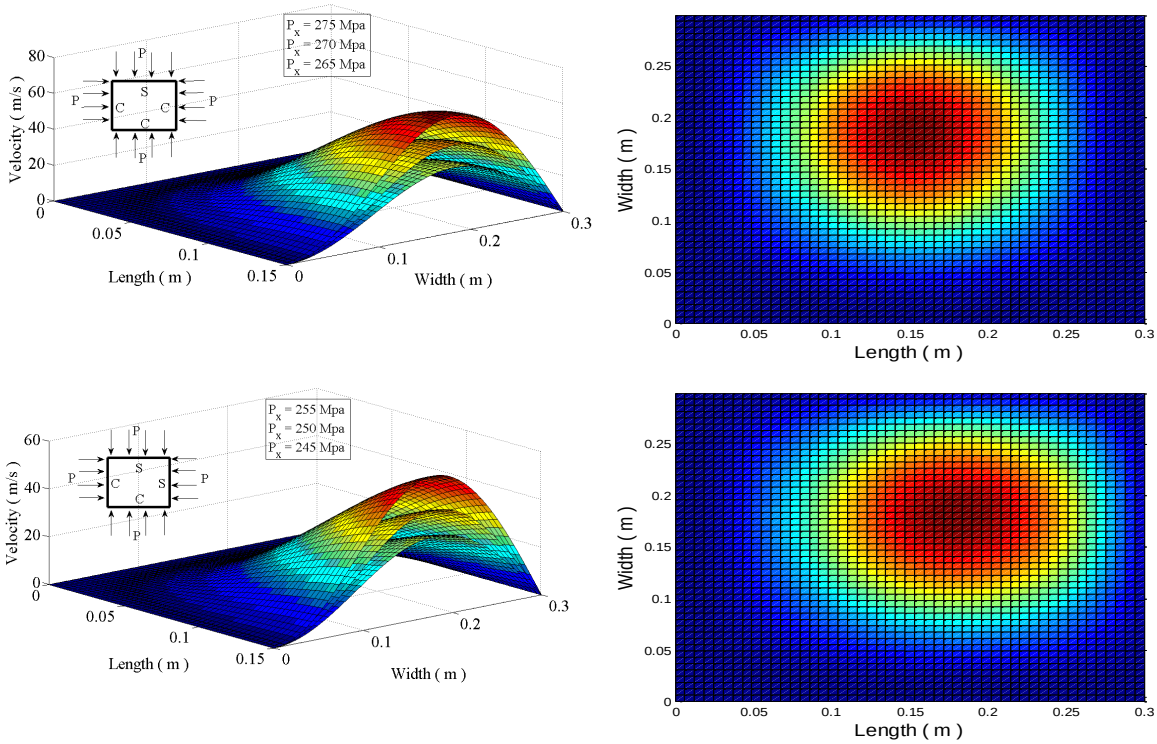

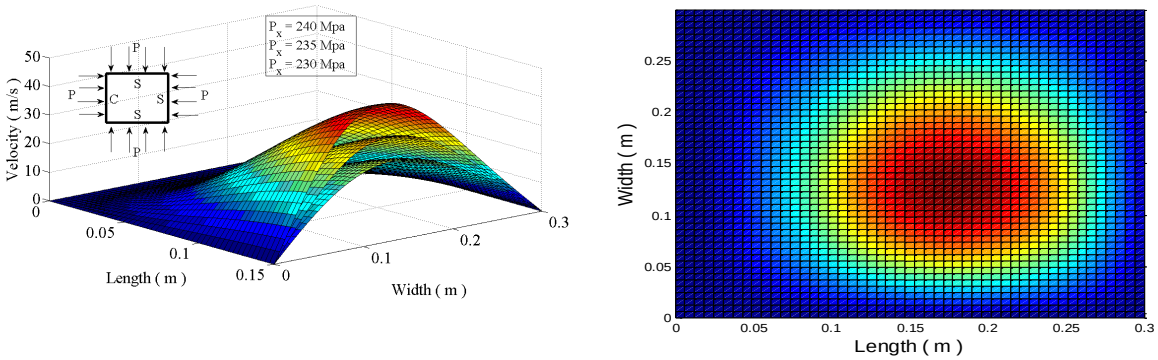

Fig. 11. Maximum velocity field of square plate with asymmetric boundary conditions subjected to biaxial different pulse amplitude.

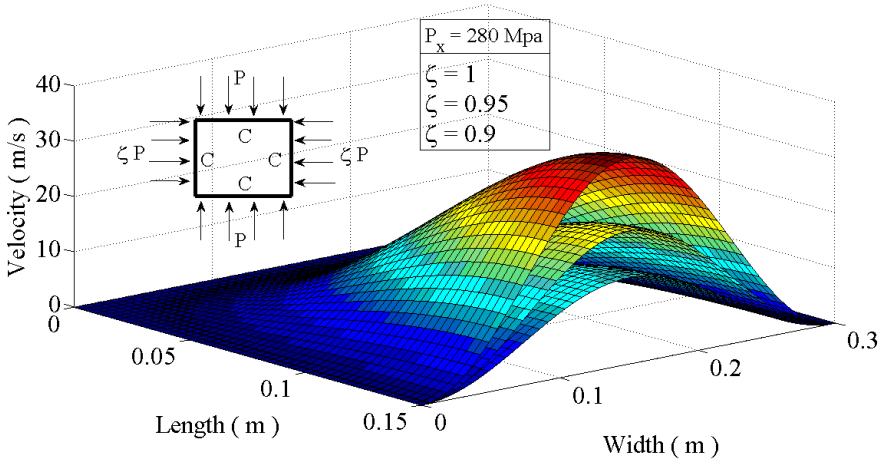

Fig. 12. Effect of loading ratio on maximum velocity field of square plate subjected to pulse amplitude

Finally, the effect of loading ratio, i.e. $\xi = 1, \xi = 0.95$, $\xi = 0.9$, on the velocity field of fully clamped square plate under sinusoidal impulsive load is depicted in Fig. 12. According to Fig. 12, it can be concluded that decreasing the aspect ratio leads to reducing of the velocity field, as the impulsive load with similar amplitude is applied.

5. Coclusion

This paper was aimed at analyzing the elastoplastic dynamic buckling of a rectangular plate exposed to uni- and biaxial compression sinusoidal pulse functions using Galerkin method and applying trigonometric mod shape functions. For this purpose, first of all, using deformation theory of plasticity (DT) with the Hencky constitutive relations and incremental theory of plasticity (IT) with the Prandtl-Reuss constitutive relations, the equilibrium, stability and dynamic elastoplastic buckling equations for rectangular plate were derived. The Ramberg-Osgood stress-strain model was used to describe the elastoplastic material property of plate. The effects of boundary conditions, force pulse amplitude, load and type of plasticity theory on the velocity and deflection histories of plate were investigated. According to the dynamic response of plate, the DT gives more accurate results than those obtained from the IT. The resistance against deformation for corresponding to plates with clamped boundary condition is more than those plates with simply supported boundary condition. Consequently, the adjacent points to clamped boundary condition have lower velocity field than those adjacent points to simply supported boundary condition.

References

[1] L.H. Mitchell, A.K. Head, 1961, The buckling of a dislocated plate, Journal of the Mechanics and Physics of Solids 9, pp. 131-139.

[2] K.C. Rockey, I.T. Cook, 1965, The buckling under pure bending of a plate girder reinforced by multiple longitudinal stiffeners, International Journal of Solids and Structures 1, pp. 147-156.

[3] A. Weinstein, 1968, The buckling of plates and beams by the method of zero lagrangian multipliers and zero divisors, International Journal of Solids and Structures 4, pp. 579-583.

[4] A. Rothwell, 1969, Optimum fiber orientations for the buckling of thin plates of composite material, Fiber Science and Technology 2, pp. 111-122.

[5] A.L. Yettram, E.S. Awadalla, 1970, The distribution of transverse reactive forces at the edges of a rectangular plate at the buckling load, International Journal of Mechanical Sciences 12, pp. 669-674.

[6] S. Srinivas, A.K. Rao, 1970, Bending vibration and buckling of simply supported thick orthotropic rectangular plates and laminates, International Journal of Solids and Structures 6, pp. 1463-1481.

[7] K.C. Rockey, D.K. Bagchi, 1970, Buckling of plate girder webs under partial edge loadings, International Journal of Mechanical Sciences 12, pp. 16-76.

[8] M.J. Sewell, 1973, A yield surface corner lowers the buckling stress of an elastic plastic plate under compression, Journal of the Mechanics and Physics of Solids 21, pp. 19-45.

[9] M. Uenoya, R.G. Redwood, 1978, Elastoplastic shear buckling of square plateswith circular holes**,** Computers and Structures 8, pp. 291-300.

[10] S.C. Shrivastava, 1979, Inelastic analysis of plates including shear effects,International Journal of Solids and Structures 15, pp. 567-575.

[11] E. Ore, D. Durban, 1989, Elastoplastic buckling of annular plates in pure shear, Journal of Applied Mechanics 56, pp. 644-651.

[12] D. Durban, Z. Zuckerman, 1999, Elastic plastic buckling of rectangular plates in biaxial compression tension, International Journal of Mechanical Sciences 41, pp. 751–765.

[13] C. Shijie, K.C. Hee, H. Hong, 1999, Experimental study of dynamic buckling of plates under sinusoidal slamming, International Journal of Impact Engineering 22, pp. 675-91.

[14] D. Petry, G. Fahlbusch, 2000, Dynamic buckling of thin isotropic plates subjected to in-plane impact, Thin-Walled Structures 38, pp. 267-283.

[15] C. Shijie, K.C. Hee KC, H. Hong, 2001, Numerical analysis of dynamic buckling of rectangular plates subjected to intermediate velocity impact, International Journal of Impact Engineering 25, pp. 147-167.

[16] C.M. Wang, Y. Xiang, J. Chakrabarty, 2001, Elasticplastic buckling of thick plates, International Journal of solids and structures 38, pp. 8617-8640.

[17] D. Karagiozova, N. Jones, 2004, Dynamic buckling of elastic–plastic square tubes under axial impact II: structural response, International Journal of Impact Engineering 30, pp. 167-192.

[18] M. Azhari, M.M. Saadatpour, M.A. Bradford, 2004, Inelastic local buckling of flat thin-walled structures containing thickness tapered plates,Thin-Walled Structures 42, pp. 351-368.

[19] C. Wang, T.M. Aung, 2007, Plastic buckling analysis of thick plates using P-Ritz method, International Journal of Solids and Structures 44, pp. 6239-6255.

[20] X. Wang, J. Huang, 2009, Elastoplastic buckling analyses of rectangular plate sunder biaxial loadings by the DQM, Thin-Walled Structures 47, pp. 14-20.

[21] S. Lotfi, M. Azhari, A. Heidarpour, 2011, Inelastic initial local buckling of skew thin thickness-tapered plates with and without intermediate supports using the isoparametric spline finite strip method, Thin-Walled Structures 49, pp. 1475-1482.

[22] M. Komur, 2011, Elastoplastic buckling analysis for perforated steel plates subject to uniform compression, Mechanics Research Communications 38, pp. 117-122.

[23] Z. Yao, K.J.R. Rasmussen, 2012, Inelastic local buckling behavior of perforated plates and sections under compression, Thin-Walled Structures 61, pp. 49-70.

[24] Z. Tang, D. Li, 2012, Experimental investigation of axial impact buckling response of pseudo elastic NiTi cylindrical shells, International Journal of Impact Engineering 39, pp. 28-41.

[25] Q. Fyllingen, E.C. Langmoen, M. Langseth, O.S. Hopperstad, 2012, Transition from progressive buckling to global bending of square aluminum tubes, International Journal of Impact Engineering 48, pp. 24-32.

[26] M.M. Alinia, G. Soltanieh, M. Amani, 2012, Inelastic buckling behavior of stocky plates under interactive shear and in-plane bending, Thin-Walled Structures 55, pp. 76-84.

[27] M.A. Douville, P.L. Grognec, 2013, Exact analytical solutions for the local and global buckling of sandwich beam-columns under various loadings, International Journal of Solids and Structures 50, pp. 2597-2609.

[28] M. Maarefdoust, M. Kadkhodayan, 2013, Elastoplastic buckling analysis of plates involving

free edges by deformation theory of plasticity, International Journal of Engineering 26, pp. 421-432.

[29] M. Kadkhodayan, M. Maarefdoust, 2014, Elastic plastic buckling of isotropic thin plates subjected to uniform and linearly varying in-plane loading using incremental and deformation theories, Aerospace Science and Technology 32, pp. 66-83.

[30] R. Shamass, G. Alfano, F.A. Guarracino, 2014, A numerical investigation into the plastic buckling paradox for circular cylindrical shells under axial compression, Engineering Structures 75, pp. 429-447.

[31] D. Trybuła, J. Kruzelecki, 2014, Non-standard stabilization of the postbuckling path for elastic plastic cylindrical shells under combined state of loadings, Thin-Walled Structures 77, pp. 120-128.

[32] R. Gumruk, 2014, A numerical investigation of dynamic plastic buckling behavior of thin-walled cylindrical structures with several geometries,Thin-Walled Structures 85, pp. 388-397.

[33] V. Picandet, N. Challamel, S. Hin, 2014, Buckling and postbuckling of gradient and nonlocal plasticity columns experiencing softening, International Journal of Solids and Structures 51, pp. 4052-4067.

[34] J. Chakrabarty, Applied Plasticity, Second ed. Springer; 2010.